Published in final edited form as:
Genesis. 2012 January ; 50(1): . doi:10.1002/dvg.20789.

Generation of Mice With a Conditional Allele for the Transforming Growth Factor Beta3 Gene

Thomas Doetschman[1,2], **Teodora Georgieva**[1], **Hongqi Li**[1], **Thomas D. Reed**[3], **Christina Grisham**[4], **Jacqueline Friel**[1], **Mark A. Estabrook**[1], **Connie Gard**[1], **L.P. Sanford**[1], and **Mohamad Azhar**[1,2,*]

[1]BIO5 Institute, University of Arizona, Tucson, Arizona

[2]Department of Cellular and Molecular Medicine, University of Arizona, Tucson, Arizona

[3]Intrexon Corporation, Blacksburg, Virginia

[4]Department of Molecular Genetics, University of Cincinnati College of Medicine, Cincinnati, Ohio

Summary

The transforming growth factor beta (TGFβ) pathway is involved in embryonic development and several inherited and acquired human diseases. The gene for TGFβ3 (*Tgfb3*) encodes one of the three ligands for TGF b receptors. It is widely expressed in the embryo and its mutation or misexpression is found in human diseases. *Tgfb3*$^{-/-}$ mice die at birth from cleft palate, precluding functional studies in adults. Here, we generated mice in which exon 6 of *Tgfb3* was flanked with *LoxP* sites (*Tgfb3*$^{flox/flox}$). The adult mice were normal and fertile. *EIIa-Cre*-mediated deletion of exon 6 in *Tgfb3*$^{flox/flox}$ mice efficiently generated *Tgfb3* conditional knockout (*Tgfb3*$^{cko/cko}$) mice which died at birth from the same cleft palate defect as *Tgfb3*$^{-/-}$ mice, indicating that the conditional and knockout alleles are functionally equivalent. This *Tgfb3*^{cko} allele will now enable studies of TGFβ3 function in different cell or tissue types in embryonic development and during adulthood. genesis 50:59-66, 2012.

Keywords

transforming growth factor beta; cardiovascular; cancer; craniofacial; wound healing; autoimmunity; neuromuscular

TGFb ligands are multifunctional proteins involved in tissue development and homeostasis and in tissue remodeling during disease pathogenesis and cancer (Azhar *et al*., 2003; Laverty *et al*., 2009; ten Dijke and Arthur, 2007). In mammals, there are three TGFb ligands (TGFβ1, TGFβ2 and TGFβ3). They are produced in latent forms, and upon activation they usually interact with TGFβR1 and TGFβR2 receptors in conjunction with TGFβR3 or Endoglin and induce phosphorylation of SMAD2 or SMAD3. These SMADs associate with SMAD4 and translocate to the nucleus, where in association with various co-repressors and activators they regulate the transcription of target genes. SMAD7 acts as an inhibitor of this canonical TGFb signaling. TGFβ signaling also occurs through SMAD-independent pathways.

*Correspondence to: Mohamad Azhar, 1656 E Mabel St, PO Box 245217, Tucson, AZ 85724-5217. azharm@email.arizona.edu.
Current address for Hongqi Li: DesigneRX Pharmaceuticals Inc., Vacaville, CA 95688.

Of the three TGFβ ligands, the role of TGFβ3 at the organismal level is somewhat less understood (Azhar *et al*., 2009a,b; Kaartinen *et al*., 1995; Kulkarni *et al*., 1993; Proetzel *et al*., 1995; Sanford *et al*., 1997; Shull *et al*., 1992). The importance of a better understanding of TGFβ3 function is underscored by several inherited and noninherited diseases in which it has been implicated. For example, mutations in the human *TGFB3* gene causes familial arrhythmogenic right ventricular dysplasia type 1 (ARVD1) [MIM:107970], also known as arrhythmogenic right ventricular cardiomyopathy 1 (ARVC1) (Beffagna *et al*., 2005). ARVD is an autosomaldominant disease characterized by partial degeneration of the myocardium of the right ventricle, electrical instability, and sudden death. Moreover, gene association studies show an association of cleft lip and palate (CL/P) with *TGFB3* (Lidral *et al*., 1998). Genetic polymorphisms are found in *TGFB3* in patients with hypertension (Hu *et al*., 2010) and ossification of the posterior longitudinal ligament of the spine (OPLL) (Horikoshi *et al*., 2006). *TGFB3* expression is increased in HELLP syndrome (hemolysis-elevated liver enzymes-low platelet count) (Emanuelli *et al*., 2008), and it is elevated in diseased canine mitral valves (Aupperle *et al*., 2008). TGFβ3 is critically involved in wound healing and is currently being used in a clinical trial for treatment of wounds (Laverty *et al*., 2009). It is involved in mammary gland development and post-lactational involution (Flanders and Wakefield, 2009), and it has been strongly implicated in the progression of various forms of cancer, including breast cancer (Laverty *et al*., 2009). In vitro, mouse keratinocytes are not protected against 12-*O*-tetradecanoylphorbol-13-acetate-induced cell death in its absence (Li *et al*., 1999). Finally, a recent study has identified an important role of TGFβ3 in immune tolerance and autoimmunity (Shah and Qiao, 2008). Thus, it is clear that TGFβ3 has important roles at the organismal level that need to be better understood.

Tgfb3 is expressed in several tissues during mouse embryonic development, including heart, lung, skin, and craniofacial structures. *Tgfb3* is expressed in a partially overlapping fashion to *Tgfb2* in the developing cardiovascular system (Azhar *et al*., 2003; Pelton *et al*., 1991). However, it is not clear if these ligands have any overlapping functions in cardiovascular development or function. *Tgfb3* is expressed during palatogenesis and wound healing (Laverty *et al*., 2009). Consistent with its expression in the developing palate, *Tgfb3* knockout mice ($Tgfb3^{-/-}$) develop cleft palate and die soon after birth (Kaartinen *et al*., 1995; Proetzel *et al*., 1995), precluding any further determination of *Tgfb3* function in adult mice. Thus, *Tgfb3* conditional knockout mice are necessary to advance the understanding of *Tgfb3* function not only during embryonic development, but also during tissue remodeling at postnatal and adult stages, and in the adult in cancer and in diseases of the cardiovascular and immune-related systems.

To circumvent the embryonic lethality exhibited by $Tgfb3^{-/-}$ mice, we generated $Tgfb3^{cko/cko}$ mice harboring conditional null alleles of *Tgfb3*. The *Tgfb3* gene consists of seven exons spanning 21.7 kb on mouse Chromosome 12. A Cre-LoxP strategy was used to flank exon 6 for Cre-mediated deletion (Fig. 1a-d). This method has been successfully used by us (Azhar *et al*., 2009a) and numerous other researchers (Nagy *et al*., 2009). Exon 6 in *Tgfb3* encodes the mature peptide of TGFb3. Total deletion of exon 6 in $Tgfb3^{-/-}$ embryos results in cleft palate (Kaartinen *et al*., 1995; Proetzel *et al*., 1995). Our conditional gene targeting of the *Tgfb3* locus resulted in four out of 143 G418-resistant ES cell colonies which had undergone correct homologous recombination. Several mouse chimeras were produced which transmitted the $Tgfb3^{flox}$ allele to the germline as demonstrated by Southern hybridization (Fig. 1e-f). PCR genotyping was used to distinguish $Tgfb3^{+/+}$, $Tgfb3^{+/flox}$ and $Tgfb3^{flox/flox}$ mice before weaning age (Fig. 2a). $Tgfb3^{flox/flox}$ mice that were born, were viable, fertile, and indistinguishable from wild-type littermates. $Tgfb3^{flox/flox}$ animals were born with near expected Mendelian ratio. Real time PCR analysis showed no difference in "wild-type" *Tgfb3* expression between wild-type and $Tgfb3^{flox/flox}$ mice (not shown). The design of the *Tgfb3* targeted allele permits removal of the *MC1Neo* cassette by mating to a

Flp deleter mouse line (generating the *Tgfb3*^{flox} allele) or removal of *LoxP*-flanked *Tgfb3* genomic sequence (including exon 6 and the *Frt-MC1NeopA-Frt* cassette) by mating to a Cre deleter line (generating the *Tgfb3*^{cko} allele). There are numerous publications detailing the unintended effects of the vigorously and ubiquitously expressed *PGK* promoter but not the *MC1* promoter on flanking gene expression (Pham et al., 1996; Ren et al., 2002; Scacheri et al., 2001). However, we are currently analyzing these mice for possible hypomorphic effects. Collectively, these data are consistent with the observation that the presence of the *LoxP* or *Frt-MC1NeopA-Frt* cassette does not alter TGFb3 function in *Tgfb3*$^{flox/flox}$ mice. Consequently, we decided to delete exon 6 and the *Frt-MC1NeopA-Frt* cassette in order to produce *Tgfb3*$^{cko/cko}$ mice by breeding *Tgfb3*$^{flox/flox}$ mice with *EIIa-Cre* transgenic mice. Cre recombinase is expressed in oocytes and preimplantation embryos when under the control of the adenoviral (*EIIa*) promoter (Holzenberger *et al*., 2000). Hence, this Cre driver line eliminates genes in all cells and creates a complete gene knockout. The deletion of exon 6 in *Tgfb3*$^{cko/cko}$ mice was confirmed by PCR (Fig. 2b). Real-time PCR analysis of the palatal tissues showed that there is no detectable expression of “wild-type” *Tgfb3* expression in *Tgfb3*$^{cko/}$cko embryos when compared to control wild-type embryos (Fig. 2c).

Intercrossing of *Tgfb3*$^{+/flox}$ *EIIa-Cre* mice did not produce viable *Tgfb3*^{cko} mice. Closer examination of five different litters showed that *Tgfb3*$^{cko/cko}$ mice were born in the expected Mendelian ratio but they gasped to death. PCR genotyping confirmed these findings. *Tgfb3*$^{cko/cko}$ pups could not suckle well and their stomachs had little milk. Consequently, *Tgfb3*$^{cko/cko}$ and wild-type littermate embryos were collected at E18.5 of gestation and carefully examined for cleft palate (n = 10 for *Tgfb3*$^{cko/cko}$, n = 30 for wild-type control). Interestingly, gross morphological examination of E18.5 embryos under a dissecting microscope revealed complete cleft palate or severe partial cleft palate in all ofthe *Tgfb3*$^{cko/cko}$ embryos (Fig. 3). Similar cleft palate defects were seen in *Tgfb3*$^{cko/cko}$ new born pups (not shown). There was no cleft palate in wild-type control embryos (Fig. 3a,c). Interestingly, *Tgfb3*$^{cko/cko}$ embryos exhibit the same cleft palate defects which were seen in *Tgfb3*$^{-/-}$ mice when on a C57BL/6 genetic background (Fig. 3b-d), (Kaartinen *et al*., 1995; Proetzel *et al*., 1995). This observation is consistent with the fact that we backcrossed *Tgfb3*$^{flox/flox}$ mice on to the C57BL/6 background for two generations before crossing with *EIIa-Cre* mice which were also on a C57BL/6 background. Thus, our data indicate that the *Tgfb3*^{cko} allele is functionally equivalent to the *Tgfb3* null allele.

Tgfb3$^{cko/cko}$ mice offer several opportunities. They will be useful in directly testing the role of TGFβ3 in susceptibility and pathogenesis of ARVD1, CL/P, hypertension, OPLL, valve disease, craniofacial diseases, and HELLP syndrome. These mice will facilitate TGFβ3 research in wound healing at postnatal stages. *Tgfb3*$^{cko/cko}$ mice will open up avenues to investigate the tissue-specific role of TGFb3 in mammary gland development and in post-lactational involution and breast cancer progression in postnatal mice. In addition, these mice will provide new opportunities to evaluate TGFβ3 function in various other forms of cancer. Finally, *Tgfb3*$^{cko/cko}$ mice can be used to formally test the potential involvement of TGFβ3 in the pathogenesis of numerous inherited and noninherited diseases in which mutations or dysregulation of downstream TGFβ signaling components has been implicated. For instance, genetic mutations and/or dysregulation of TGFβ pathway genes are involved in cardiovascular and muscular (valve disease, cardiac hypertrophy, cardiac fibrosis, aneurysm, hypertension, atherosclerosis) (Dietz, 2010; Shimizu *et al*., 2011; Teekakirikul *et al*., 2010; van I *et al*., 2011), skeletal and craniofacial (Lidral *et al*., 1998), ocular (Saika *et al*., 2009), neurodegenerative, and neuromuscular (Katsuno *et al*., 2011), and in fibrotic and immunological disorders and diseases (Pohlers *et al*., 2009; Shah and Qiao, 2008). In most cases it remains unclear as to which TGFβ ligand(s) are responsible for these diseases, so these mice will be useful for determining their ligand/signaling specificity.

In conclusion, we have produced a *Tgfb3*^{cko} allele and showed that it causes perinatal lethality due to cleft palate defects that phenocopy those of *Tgfb3*$^{\beta/\beta}$ mice. Thus, *Tgfb3*$^{cko/cko}$ mice provide a novel mouse strain to determine the tissue or cell-type specific roles of TGFβ3 during embryogenesis and in adult life and to investigate the mechanisms underlying TGFβ3 dysregulation in human disease.

METHODS

Generation and Phenotypic Analysis of Mice Carrying Tgfb3^{cko} Allele

All procedures are approved by the Institutional Animal Care and Use the Committee at University of Arizona. Conditional gene targeting vector for the *Tgfb3*$^{flox/flox}$ mice was produced from a mouse genomic library clone (129/J). The targeting strategy was to conditionally delete exon 6 of *Tgfb3* by using a Cre-LoxP strategy. A similar approach targeting exon 6 had been used previously to successfully produce *Tgfb3*$^{\beta/\beta}$ mice (Proetzel *et al*., 1995). A 6.5 kb KpnI genomic DNA fragment containing exon 5-7 of *Tgfb3* was subcloned in a pAC7-P7 plasmid and used for building the targeting vector (Fig. 1a-d). The left homology arm of the targeting vector was 3.1 kb. The right homology arm was 2.4 kb. Two *LoxP* sites were placed in similar orientation. The first *LoxP* site is located in intron 6. A *FrtMC1NeopA-Frt* selection cassette with two flanking *Frt* sites was inserted after this *LoxP* site in intron 6. The *MC1NeopA* cassette was flanked by *Frt* sites for removal by Flp recombinase (Farley *et al*., 2000). The second *LoxP* site was inserted 344 bp into intron 7. A diphtheria toxin cassette (*PGK-DTA*) at the 3′ terminus and an MC1 promoter-herpes simplex virus-thymidine kinase cassette (*MC1TK*) at the 5′ terminus of the gene targeting vector was introduced for negative selection against random integration of the targeting vector into the embryonic stem (ES) cell genome. The accuracy of the entire targeting vector was confirmed by DNA sequenc-ing. The *PI PspI*-linearized targeting vector was electroporated into KG-1 (129/SvEv) ES cells. ES cells were treated with G418 (225 lg/ml) and remained in this selection for the entire time they were in culture. Counter selection with Ganciclovir (2 mM) was applied for 3 days. A total of 143 ES cell colonies were picked and screened by PCR and southern blotting. Two targeted ES clones were injected into C57BL/6 x DBA2 blastocysts for generating chimeric mice. Germline transmission of the *Tgfb3*^{flox} allele was established by breeding the male ES cell chimeric mice to Black-Swiss females according to previously described methods (Azhar *et al*., 2009a). Germline transmission of the *Tgfb3*^{flox} allele was confirmed by both genomic PCR and southern blotting. The germline chimeric mice were backcrossed to C57BL/6J mice for two generations. *Tgfb3*$^{1/flox}$ mice were intercrossed to yield *Tgfb3*$^{flox/flox}$ mice. *Tgfb3*$^{+/}$flox*EIIa-Cre* mice (129/J/Black-Swiss/C57BL/6) were generated by crossing *Tgfb3*$^{flox/flox}$ (129/Black-Swiss/ C57BL/6) to *EIIa-Cre* mice (C57BL/6) (Jax Lab, Bar harbor, ME). Timed-pregnant *Tgfb3*$^{1/flox}$ *EIIa-Cre* intercrossed mice were used to collect E18.5 wild-type and *Tgfb3*$^{flox/flox}$ *EIIa-Cre* embryos in which the *Tgfb3*^{flox} allele should have been converted to the *Tgfb3*^{cko} allele. All embryos were examined for cleft palate under a stereozoom dissecting microscope (Zeiss Inc.) and digitally photographed. Tail clips were used to extract genomic DNA (Invitrogen Inc.) for PCR genotyping of embryos. Non-transgenic *EIIa-Cre* littermates which were *Tgfb3*$^{flox/flox}$ or *Tgfb3*$^{+/+}$ *EIIa-Cre* were used as control animals. PCR analysis on tail clip DNA was used for genotyping *Tgfb3*$^{cko/cko}$ mice. The following PCR primers were used for genotyping: AGATAAACAATGGAGTCT GTCATGG (*Tgfb3* forward primer, p1), TTCTGGATTC ATCGACTGTGG (*Neomycin*, reverse primer, p2), GTC TCATATGTGTCTTCCTGTCTCC (*Tgfb3* reverse primer, p3); PCR conditions (Denaturation, 95°C/90 sec; Amplification, 57°C/50 sec, 72°C/60 sec, 95°C/30 sec for 34 cycles, 57°C/50 sec, 72°C/5 min, 28°C/10 min).

Southern Hybridization, DNA Sequencing, and PCR Analyses

For southern hybridization, mouse tail genomic DNA samples (30 μg) were digested with restriction endonucleases and electrophoresed in 0.7% agarose gels. DNA was transferred to positively charged nylon membrane (Roche Applied Science Inc.) by capillary blotting and crosslinked by UV irradiation. For probe labeling, 5′-end and 3′-end digoxygenin (DIG)-labeled southern blot probes were prepared by PCR procedure using *Taq* DNA polymerase and incorporating DIG-11-dUTP according to the procedures described by the manufacturer (Roche Applied Science Inc.). The following primers were used to amplify the 5′-end (1.0 kb) probe: AATTGAACTCTGCTCTATTGCTTGC (forward primer) and GGAAGTGAGTTATATTCAGAGTCATGG (reverse primer). For the 3′-end (0.9 kb probe), the following primers were used: AGCTTAGATGTGCTTCTCAATG ACC (forward primer) and CTTCAGCAGACCTAGTCAT TGTAGTCC (reverse primer). Genomic DNA (50 ng) was used as template in the reaction. The synthesis of the labeled probes was examined on a gel. The labeled probe was clearly distinguished from the unlabeled probe since it migrated slower than the unlabeled probe. The manufacturer's recommended probe concentration of 10-20 ng/ml was used in the blot hybridizations. Following prehybridization in 10 ml of DIG EasyHyb solution at 42°C for 1 h, hybridization was carried out at 42°C overnight in a hybridization oven. The membranes were then washed 2-3 times in 2x standard sodium citrate (SSC), 0.1% sodium dodecyl sulfate (SDS) at room temperature for 5 min each and twice in 0.1x SSC, 0.1% SDS at 68°C for 15-20 min each. Detection of the hybridized probe DNA was carried out as described in the Manufacturer's User Guide. CSPD chemiluminescent substrate was used and signals were visualized on X-ray film after 5-30 min.

Automated DNA sequencing of PCR-amplified products was used to confirm the sequence accuracy and correct orientation of the *Frt-MC1NeopA-Frt* cassette and *LoxP* and *Frt* sequences in all targeted ES cell clones and *Tgfb3*$^{cko/cko}$ mice. The following combination of PCR and DNA sequencing primers were used to confirm the sequence orientation of *LoxP* and *FrtMC1NeopA-Frt* cassette located in intron 6: For PCR amplification, GTCACACCTTTCAGCCCAAT (forward primer); CGTGCTATGGGTTGTGTCTG (reverse primer); sequencing primers, TCGCCTTCTTGACGAGTTCT; AAA ACCACACTGCTCGACAT; AGGATCTCCTGTCATCTCAC CTTGCTCCTG. The following primers for amplification and sequencing of the second *LoxP* located downstream to exon 6 were used: For PCR amplification, AAATGGGT CCACGAACCTAA (forward primer); CGTGCTATGGGTT GTGTCTG (reverse primer); sequencing primer, ATGCT TAGTGTGTGCCATGC.

Genomic PCR was used to detect the *Tgfb3*^{cko} allele after Cre-mediated excision of exon 6 in the *Tgfb3*^{flox} allele. Specific primers that were used for the PCR amplification included: AGATAAACAATGGAGTCTGTCATGG (forward primer, p1), GTCTCATATGTGTCTTCCTGTCT CC (*Tgfb3* reverse primer, p3), AAGGTCTTCCTGTCTG TAAGTTTCC (*Tgfb3* reverse primer, p4); PCR conditions (denaturation: 95°C/3 min, annealing and amplification 95°C/30 sec, 64°C/1 min, 72°C/2 min for 35 cycles, 72°C/10 min).

Real-Time PCR Analysis

Various tissues (heart, lung, liver, intestine, kidney, lower and upper jaws, and skin) were collected in RNA. Later RNA stabilization solution (Qiagen Inc., Valencia, CA) from both control and *Tgfb3*$^{flox/flox}$ *EIIa-Cre*-generated embryos at E18.5. Total RNA was extracted by RNeasy Mini kit (Cat# 74104: Qiagen, Valencia, CA). RNA was DNase treated with TURBO-DNA free kit (Ambion). cDNA was transcribed using the iScript cDNA Synthesis Kit (Bio-Rad, Richmond, CA). cDNA concentration was measured using fluorometry

(Turner Biosystems) after staining with Quant-iT™ OliGreen® ssDNA Assay Kit (# O11492, Molecular Probes). Equal amounts of cDNA samples from more than three control or experimental embryos were assessed (each in triplicate) by both RT-PCR and real time PCR analyses, as described (Azhar *et al*., 2009a,b). FastStart SYBR Green Master (Roche) mix was used for real time PCR analysis. Real-time PCR analysis was carried out in the Rotor Gene 3000 System from Corbett Research. Analysis of the data was carried out using the Rotor Gene 6 software. All real-time PCR results were normalized to the housekeeping gene *Gapdh*. Primers that were used for real time PCR amplification of *Tgfb3* included: *Tgfb3* exon 4 forward, GTCACACCTTTCAGCCCAAT; *Tgfb3* exon 6 reverse, CGTGCTATGGGTTGTGTCTG; *Gapdh* forward, TGACCACAGTCCATGCCATC; *Gapdh* reverse, GACGGACACATTGGGGGTAG. Microsoft Excel was used for managing the data. Findings were reported as means ± SD of the mean, and two-tailed Student's *t*-test (SigmaPlot, Systat Software, Inc., CA) was used for comparing groups. *P*-values were calculated, and a $P < 0.05$ was considered significant.

Acknowledgments

We thank The Gene Targeted Mouse Service at the University of Cincinnati College of Medicine and The Genetically Engineered Mouse Modeling Core at the BIO5 Institute of the University of Arizona for generating chimeric *Tgfb3*^{flox} animals and PCR/Southern blot screening of *Tgfb3*^{flox} mice, respectively. Supported by NIH grants AI067903, HL092508 and CA084291 to TD.

Contract grant sponsor: National Institutes of Health Grants; Contract grant numbers: HL070174 and HL92508; Contract grant sponsor: Arizona Biomedical Research Commission; Contract grant numbers: ABRC #0901; Contract grant sponsor: The Stephen Michael Schneider/The William J. "Billy" Gieszl Award

LITERATURE CITED

Aupperle H, Marz I, Thielebein J, Schoon HA. Expression of transforming growth factor-beta1, -beta2 and -beta3 in normal and diseased canine mitral valves. J Comp Pathol. 2008; 139:97–107. [PubMed: 18640684]

Azhar M, Runyan RB, Gard C, Sanford LP, Miller ML, Andringa A, Pawlowski S, Rajan S, Doetschman T. Ligand-specific function of transforming growth factor beta in epithelial-mesenchymal transition in heart development. Dev Dyn. 2009b; 238:431–442. PMC2805850. [PubMed: 19161227]

Azhar M, Schultz JE, Grupp I, Dorn GW, Meneton P, Molin DG, Gittenberger-de Groot AC, Doetschman T. Transforming growth factor beta in cardiovascular development and function. Cytokine Growth Factor Rev. 2003; 14:391–407. [PubMed: 12948523]

Azhar M, Yin M, Bommireddy R, Duffy JJ, Yang J, Pawlowski SA, Boivin GP, Engle SJ, Sanford LP, Grisham C, Singh RR, Babcock GF, Doetschman T. Generation of mice with a conditional allele for transforming growth factor beta 1 gene. Genesis. 2009a; 47:423–431. [PubMed: 19415629]

Beffagna G, Occhi G, Nava A, Vitiello L, Ditadi A, Basso C, Bauce B, Carraro G, Thiene G, Towbin JA, Danieli GA, Rampazzo A. Regulatory mutations in transforming growth factor-beta3 gene cause arrhythmogenic right ventricular cardiomyopathy type 1. Cardiovasc Res. 2005; 65:366–373. [PubMed: 15639475]

Dietz HC. TGF-beta in the pathogenesis and prevention of disease: A matter of aneurysmic proportions. J Clin Invest. 2010; 120:403–407. [PubMed: 20101091]

Emanuelli M, Giannubilo SR, Landi B, Sartini D, Pierella F, Corradetti A, Tranquilli AL. Placental overexpression of transforming growth factor-beta3 in the HELLP syndrome. Gynecol Obstet Invest. 2008; 65:1–5. [PubMed: 17671384]

Farley FW, Soriano P, Steffen LS, Dymecki SM. Widespread recombinase expression using FLPeR (flipper) mice. Genesis. 2000; 28:106–110. [PubMed: 11105051]

Flanders KC, Wakefield LM. Transforming growth factor-(beta)s and mammary gland involution: Functional roles and implications for cancer progression. J Mammary Gland Biol Neoplasia. 2009; 14:131–144. [PubMed: 19396528]

Holzenberger M, Lenzner C, Leneuve P, Zaoui R, Hamard G, Vaulont S, Bouc YL. Cre-mediated germline mosaicism: A method allowing rapid generation of several alleles of a target gene. Nucleic Acids Res. 2000; 28:E92. [PubMed: 11058142]

Horikoshi T, Maeda K, Kawaguchi Y, Chiba K, Mori K, Koshizuka Y, Hirabayashi S, Sugimori K, Matsumoto M, Kawaguchi H, Takahashi M, Inoue H, Kimura T, Matsusue Y, Inoue I, Baba H, Nakamura K, Ikegawa S. A large-scale genetic association study of ossification of the posterior longitudinal ligament of the spine. Hum Genet. 2006; 119:611–616. [PubMed: 16609882]

Hu BC, Li L, Sun RH, Gao PJ, Zhu DL, Wang JG, Chu SL. The association between transforming growth factor beta3 polymorphisms and left ventricular structure in hypertensive subjects. Clin Chim Acta. 2010; 411:558–562. [PubMed: 20083094]

Kaartinen V, Voncken JW, Shuler C, Warburton D, Bu D, Heisterkamp N, Groffen J. Abnormal lung development and cleft palate in mice lacking TGF-beta 3 indicates defects of epithelial-mesenchymal interaction. Nat Genet. 1995; 11:415–421. [PubMed: 7493022]

Katsuno M, Adachi H, Banno H, Suzuki K, Tanaka F, Sobue G. Transforming growth factor-beta signaling in motor neuron diseases. Curr Mol Med. 2011; 11:48–56. [PubMed: 21189118]

Kulkarni AB, Huh CG, Becker D, Geiser A, Lyght M, Flanders KC, Roberts AB, Sporn MB, Ward JM, Karlsson S. Transforming growth factor beta 1 nullmutation in mice causes excessive inflammatory response and early death. Proc Natl Acad Sci USA. 1993; 90:770–774. [PubMed: 8421714]

Laverty HG, Wakefield LM, Occleston NL, O'Kane S, Ferguson MW. TGF-beta3 and cancer: A review. Cytokine Growth Factor Rev. 2009; 20:305–317. [PubMed: 19656717]

Li J, Foitzik K, Calautti E, Baden H, Doetschman T, Dotto GP. TGF-beta3, but not TGF-beta1, protects keratinocytes against 12-*O*-tetradecanoylphorbol-13-acetate-induced cell death in vitro and in vivo. J Biol Chem. 1999; 274:4213–4219. [PubMed: 9933619]

Lidral AC, Romitti PA, Basart AM, Doetschman T, Leysens NJ, Daack-Hirsch S, Semina EV, Johnson LR, Machida J, Burds A, Parnell TJ, Rubenstein JL, Murray JC. Association of MSX1 and TGFB3 with nonsyndromic clefting in humans. Am J Hum Genet. 1998; 63:557–568. [PubMed: 9683588]

Nagy A, Mar L, Watts G. Creation and use of a cre recombinase transgenic database. Methods Mol Biol. 2009; 530:365–378. [PubMed: 19266338]

Pelton RW, Saxena B, Jones M, Moses HL, Gold LI. Immunohistochemical localization of TGF beta 1, TGF beta 2, and TGF beta 3 in the mouse embryo: Expression patterns suggest multiple roles during embryonic development. J Cell Biol. 1991; 115:1091–1105. [PubMed: 1955457]

Pham CT, MacIvor DM, Hug BA, Heusel JW, Ley TJ. Long-range disruption of gene expression by a selectable marker cassette. Proc Natl Acad Sci USA. 1996; 93:13090–13095. [PubMed: 8917549]

Pohlers D, Brenmoehl J, Loffler I, Muller CK, Leipner C, Schultze-Mosgau S, Stallmach A, Kinne RW, Wolf G. TGF-beta and fibrosis in different organs - Molecular pathway imprints. Biochim Biophys Acta. 2009; 1792:746–756. [PubMed: 19539753]

Proetzel G, Pawlowski SA, Wiles MV, Yin M, Boivin GP, Howles PN, Ding J, Ferguson MW, Doetschman T. Transforming growth factor-beta 3 is required for secondary palate fusion. Nat Genet. 1995; 11:409–414. [PubMed: 7493021]

Ren SY, Angrand PO, Rijli FM. Targeted insertion results in a rhombomere 2-specific Hoxa2 knock-down and ectopic activation of Hoxa1 expression. Dev Dyn. 2002; 225:305–315. [PubMed: 12412013]

Saika S, Yamanaka O, Okada Y, Tanaka S, Miyamoto T, Sumioka T, Kitano A, Shirai K, Ikeda K. TGF beta in fibroproliferative diseases in the eye. Front Biosci (Schol Ed). 2009; 1:376–390. [PubMed: 19482708]

Sanford LP, Ormsby I, Gittenberger-de GA, Sariola H, Friedman R, Boivin GP, Cardell EL, Doetschman T. TGFbeta2 knockout mice have multiple developmental defects that are non-overlapping with other TGFbeta knockout phenotypes. Development. 1997; 124:2659–2670. [PubMed: 9217007]

Scacheri PC, Crabtree JS, Novotny EA, Garrett-Beal L, Chen A, Edgemon KA, Marx SJ, Spiegel AM, Chandrasekharappa SC, Collins FS. Bidirectional transcriptional activity of PGK-neomycin and unexpected embryonic lethality in heterozygote chimeric knockout mice. Genesis. 2001; 30:259–263. [PubMed: 11536432]

Shah S, Qiao L. Resting B cells expand a CD41CD251Foxp31 Treg population via TGF-beta3. Eur J Immunol. 2008; 38:2488–2498. [PubMed: 18792402]

Shimizu C, Jain S, Davila S, Hibberd ML, Lin KO, Molkara D, Frazer JR, Sun S, Baker AL, Newburger JW, Rowley AH, Shulman ST, Davila S, Burgner D, Breunis WB, Kuijpers TW, Wright VJ, Levin M, Eleftherohorinou H, Coin L, Popper SJ, Relman DA, Fury W, Lin C, Mellis S, Tremoulet AH, Burns JC. Transforming growth factor-{beta} signaling pathway in patients with Kawasaki disease. Circ Cardiovasc Genet. 2011; 4:16–25. [PubMed: 21127203]

Shull MM, Ormsby I, Kier AB, Pawlowski S, Diebold RJ, Yin M, Allen R, Sidman C, Proetzel G, Calvin D, Doetschman T. Targeted disruption of the mouse transforming growth factor-beta 1 gene results in multifocal inflammatory disease. Nature. 1992; 359:693–699. [PubMed: 1436033]

Teekakirikul P, Eminaga S, Toka O, Alcalai R, Wang L, Wakimoto H, Nayor M, Konno T, Gorham JM, Wolf CM, Kim JB, Schmitt JP, Molkentin JD, Norris RA, Tager AM, Hoffman SR, Markwald RR, Seidman CE, Seidman JG. Cardiac fibrosis in mice with hypertrophic cardiomyopathy is mediated by non-myocyte proliferation and requires Tgf-beta. J Clin Invest. 2010; 120:3520–3529. [PubMed: 20811150]

ten Dijke P, Arthur HM. Extracellular control of TGFbeta signalling in vascular development and disease. Nat Rev Mol Cell Biol. 2007; 8:857–869. [PubMed: 17895899]

van dL I, Oldenburg RA, Pals G, Roos-Hesselink JW, de Graaf BM, Verhagen JM, Hoedemaekers YM, Willemsen R, Severijnen LA, Venselaar H, Vriend G, Pattynama PM, Collee M, Majoor-Krakauer D, Poldermans D, Frohn-Mulder IM, Micha D, Timmermans J, Hil-horst-Hofstee Y, Bierma-Zeinstra SM, Willems PJ, Kros JM, Oei EH, Oostra BA, Wessels MW, Bertoli-Avella AM. Mutations in SMAD3 cause a syndromic form of aortic aneurysms and dissections with early-onset osteoarthritis. Nat Genet. 2011; 43:121–126. [PubMed: 21217753]

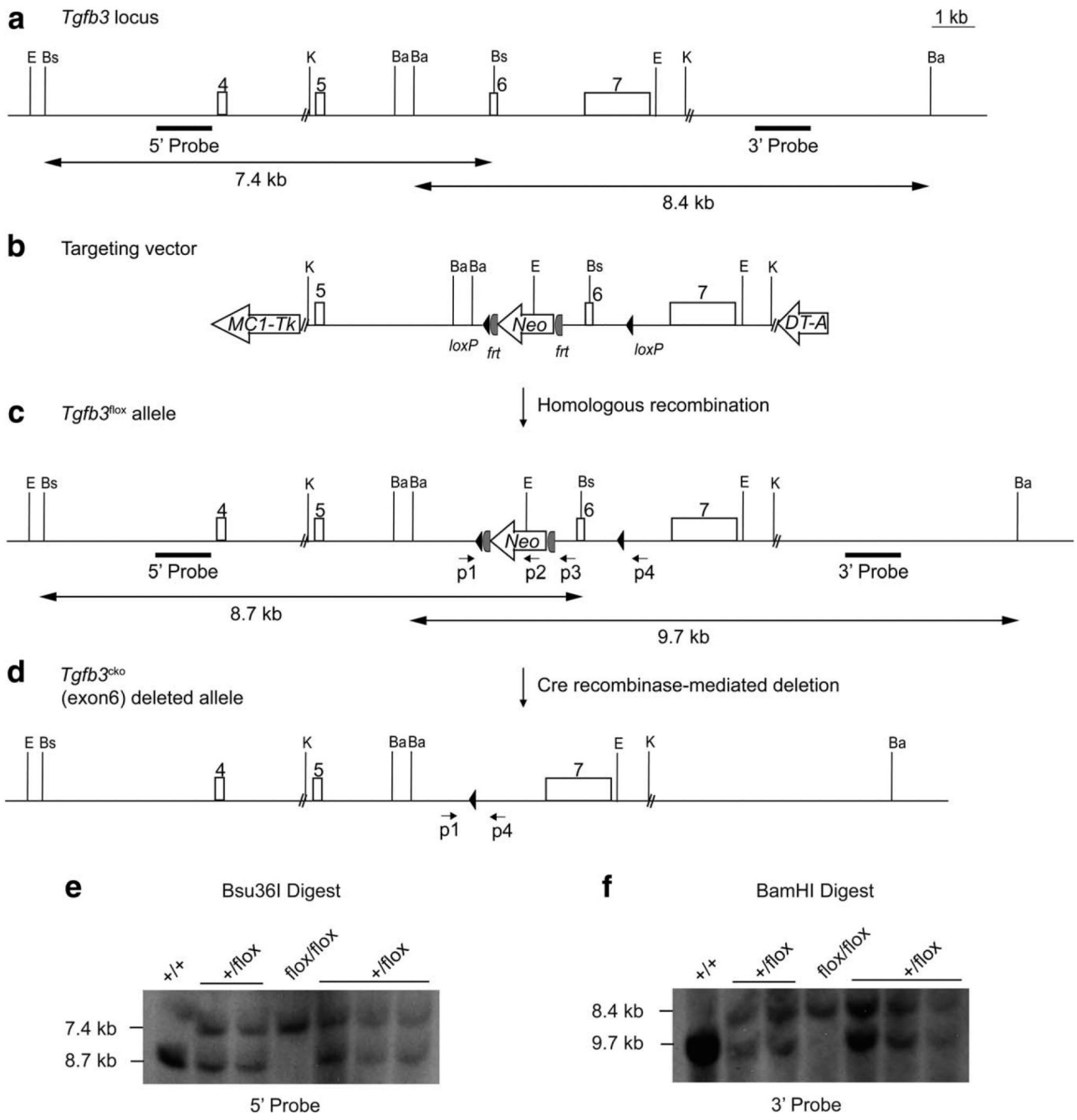

FIG. 1.

Conditional gene targeting scheme for generating *Tgfb3*^{flox} mice. **a:** Schematic diagram of the *Tgfb3* wild-type genomic locus depicting the genomic region from intron 4 to the 3′ untranslated region. Boxes with numbers on top represent exons. Both 5′ outside and 3′ outside probes and the expected band sizes used for Southern blot screening of targeted *Tgfb3*^{flox}ES cell colonies are indicated. Restriction enzymes that are used in Southern hybridization are also highlighted in abbreviated form: E, EcoRI; Bs, Bsu36I; K, KpnI; Ba, BamHI. **b:** Conditional gene targeting vector. The targeting vector consists of a KpnI genomic DNA fragment which contains *Tk-MC1* negative selection gene, 5′ or left homology arm, a *LoxP* site followed by a *Frt-MC1NeopA-Frt* cassette in intron 6, another

LoxP site in intron 7, 3′ or right homology arm, and a *PGK-DTA* expression cassette. **c:** Schematic representation of targeted *Tgfb3*^{flox} allele. Southern hybridization probes and PCR screening and genotyping primers are indicated. **d:** Schematic diagram depicting Cre-mediated recombination of the *Tgfb3*^{flox} allele to yield the *Tgfb3*^{cko} allele. Primers that identify the Cre-deletion events are indicated. **e:** Southern hybridization screening showing successful generation of wild-type, *Tgfb3*$^{+/flox}$ and *Tgfb3*$^{flox/flox}$ animals. Genomic DNA from tail clips is digested with Bsu36I and probed with the external probe (5′ Probe). Bsu36I cuts in the 5′ outside region of Tgfb3 and inside the targeting vector. Wild-type mice show an expected 8.7 kb band. Both *Tgfb3*$^{+/flox}$ and *Tgfb3*$^{flox/flox}$ animals show expected and correctly targeted bands of 8.7 kb and 7.4 kb, and 7.4 kb, respectively. **f:** BamHI digest probed with an external probe (3′ Probe) confirms the presence of *Tgfb3*$^{+/flox}$ (9.7 kb and 8.4 kb) and *Tgfb3*$^{flox/flox}$ (8.4 kb) mice. Wild-type mice show the expected 9.7 kb band.

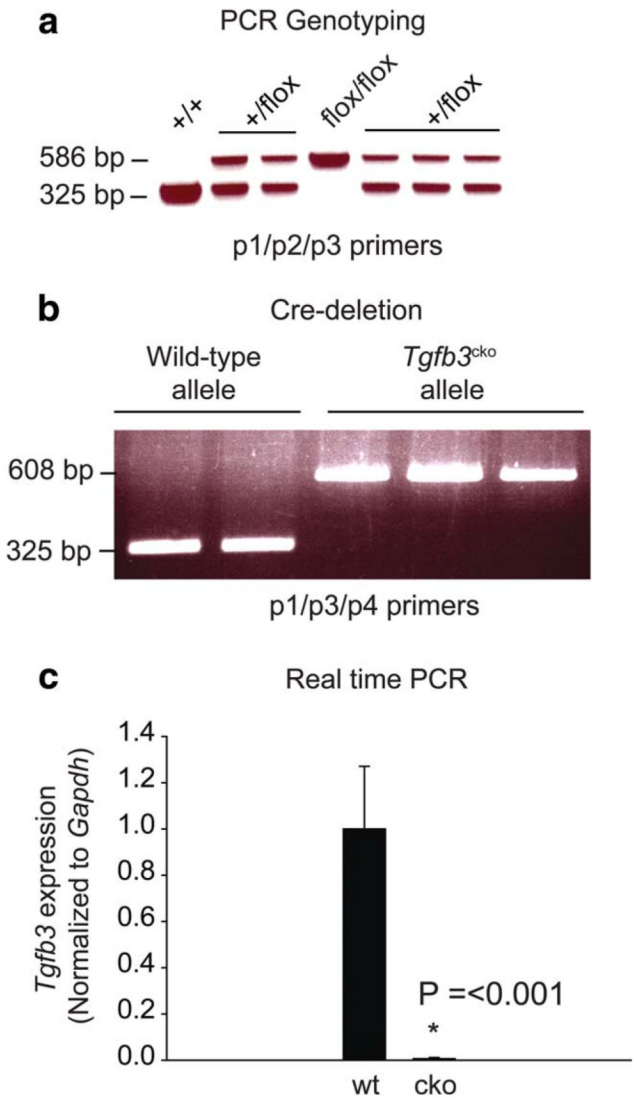

FIG. 2.

Generation of mice harboring *Tgfb3*^{cko} allele. **a:** PCR genotyping of mice with *Tgfb3*^{flox} allele. The primers used are: p1 (intron 6 *forward* primer), p2 (Neo *reverse* primer), and p3 (intron 6 *reverse* primer). The p1 and p3 primers produce a PCR product of 325 bp from the wild-type allele, whereas p1 and p2 primers give rise to a PCR product of 586 bp from the *Tgfb3*^{flox} allele. Band size as measured by DNA size markers is indicated. +/+, wild-type; +/flox, *Tgfb3*$^{+/flox}$; flox/flox, *Tgfb3*$^{flox/flox}$. **b:** Cre-mediated deletion in *Tgfb3*$^{flox/flox}$ EIIa-Cre embryos (i.e., embryos with *Tgfb3*^{cko} alleles) at E18.5. Tgfb3$^{+/+}$ *EIIa-Cre* embryos were used as wild-type controls. The primers used are p1 (intron 6 *forward* primer), p3 (intron 6 *reverse* primer), and p4 (intron 7 *reverse* primer). Genomic DNA extracted from the palate tissue is used for PCR analysis. Briefly, the p1 and p3 primers produce a PCR product of 325 bp from the wild-type allele, whereas p1 and p3 primers amplify a PCR product of 1246 bp from the undeleted *Tgfb3*^{flox} allele. The p1 and p4 primers results in a PCR product of 608 bp from the *Tgfb3*^{cko} allele. Notably, *Tgfb3*$^{+/+}$ *EIIa-Cre* embryos show a PCR product of 325 bp (i.e., expected band size of a wild-type allele) and that *Tgfb3*$^{flox/}$flox *EIIa-Cre* embryos give rise to a 608 bp PCR product (i.e., expected band size of a *Tgfb3*^{cko} allele). There was no detectable 1246 bp band (i.e., expected band size of an undeleted *Tgfb3*^{flox}

allele) in the *Tgfb3*$^{flox/flox}$ *EIIa-Cre* embryos, indicating a complete deletion of both *Tgfb3*^{flox} alleles (i.e., presence of *Tgfb3*^{cko} alleles) in *Tgfb3*$^{flox/flox}$ *EIIa-Cre* embryos. **c:** Real time PCR analysis of "wild-type" *Tgfb3* expression in wild-type control and *Tgfb3*^{cko} embryos at E18.5. Total RNA from palate tissue is used to prepare the cDNA. *Tgfb3* exon 4 forward and *Tgfb3* exon 6 reverse primers are used for real time PCR analysis. Note that there is no detectable "wild-type" Tgfb3 expression in palate tissue of *Tgfb3*^{cko} embryos (**P* = <0.001, *n* = 5 for wild-type, *n* = 3 for *Tgfb3*^{cko}). Expression levels are normalized to Gapdh and to the wild-type value.

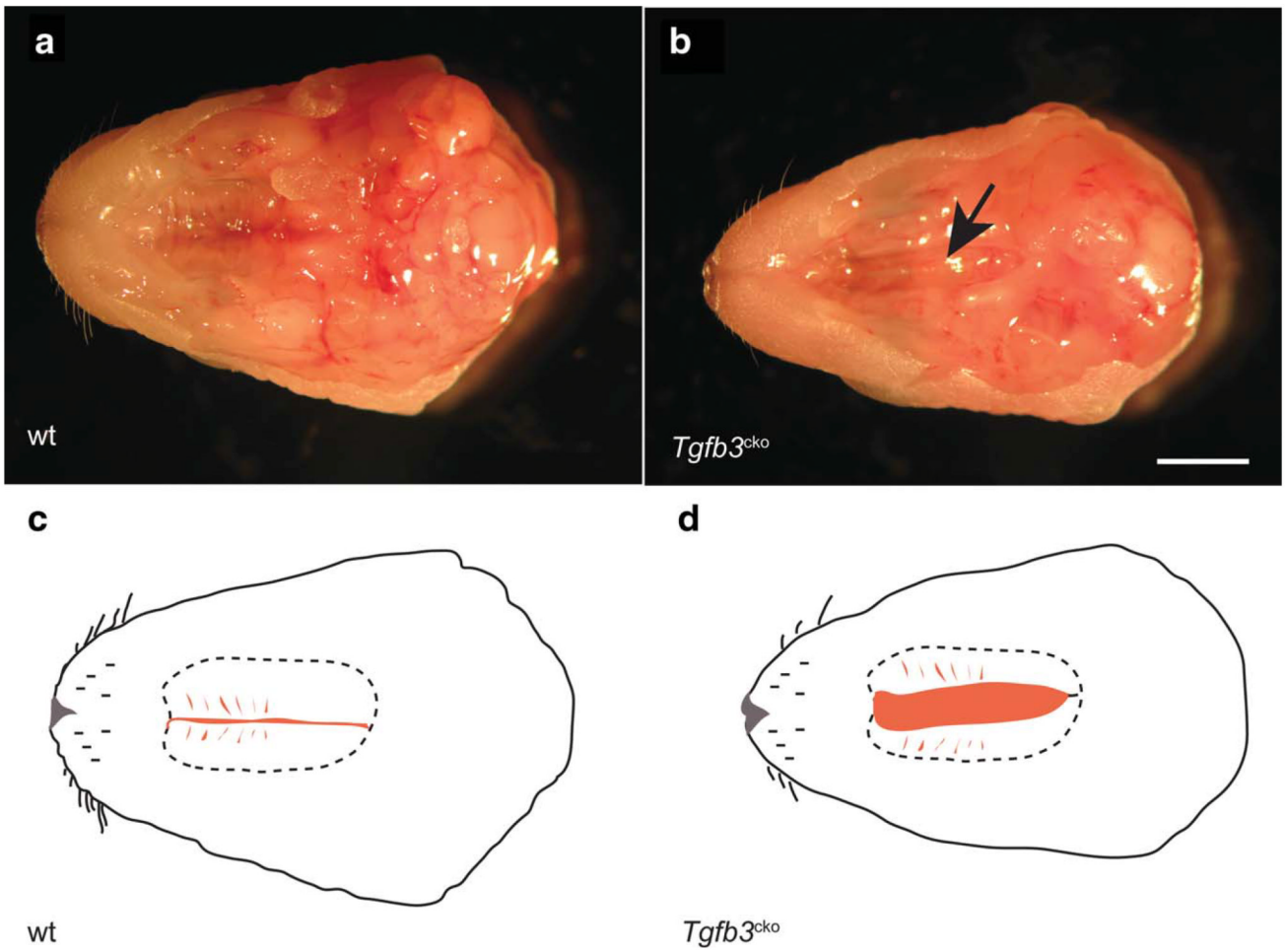

FIG. 3.

Conditional deletion of *Tgfb3* causes cleft palate in embryos. **a:** Gross morphological examination of a wild-type embryo (E18.5) showing normally fused palatal shelves. **b:** A *Tgfb3*$^{flox/flox}$ *EIIa-Cre* (i.e., *Tgfb3*^{cko}) embryo at E18.5 exhibits a cleft palate (arrow). **c,d:** Diagrammatic representation of normal palatal shelves of a wild-type (C) and the cleft palate of a *Tgfb3*^{cko} (D) embryo.